

THE PHYSICAL REVIEW

A journal of experimental and theoretical physics established by E. L. Nichols in 1893

SECOND SERIES, VOL. 89, No. 2

JANUARY 15, 1953

Distribution in Energy of the Neutrons from the Interaction of 14-Mev Neutrons with Some Elements*

ELIZABETH R. GRAVES AND LOUIS ROSEN

University of California, Los Alamos Scientific Laboratory, Los Alamos, New Mexico

(Received October 6, 1952)

The neutron spectra from the interaction of 14-Mev neutrons with a number of elements have been determined by nuclear plate techniques. The plates were exposed to neutrons from the bombardment of a Zr-T target by 200-kev deuterons when the target was as nearly as possible isolated from all scattering material and when the target was surrounded by a spherical shell of the element to be investigated. The variation of $F(E_n)$, the number of emitted neutrons per unit energy interval with energy (E_n), appears to be Maxwellian in the region 0.5 to 4.0 Mev and may be represented by

$$F(E_n)dE_n = CE_n e^{-E_n/T} dE_n.$$

I. INTRODUCTION

THERE now exist considerable experimental data on the inelastic scattering of fast neutrons by various elements. However, very few of the experiments permit a detailed evaluation of the absolute cross section for inelastic scattering as a function of the energy of the emitted neutrons.

Barschall *et al.*¹ investigated the inelastically scattered neutrons from a number of different elements and for several incident neutron energies below 3.0 Mev. By counting proton recoils in a proportional counter, they measured the cross section for inelastic scattering to below predetermined energies which were varied from 0.4 to 2.25 Mev. These data were interpreted by Feld² in terms of the statistical theory of Weisskopf and co-workers³ and also in terms of individual levels. Feld found that, although the inelastic scattering of tungsten at these low excitation energies agrees quite well with the statistical theory, the data on iron and lead cannot readily be so interpreted, but do lend themselves to interpretation in terms of an individual level theory,

applicable when only a few levels of the target nucleus are involved.

Gittings *et al.*⁴ performed an experiment in which the cross sections for inelastic collision of 14.5-Mev neutrons with lead were measured by Al(n,p) and Cu($n,2n$) detectors. Similar measurements were made by Phillips *et al.*,⁵ with the addition of P(n,p) detectors, for a number of elements. Both investigations indicated that secondary neutrons, i.e., inelastically scattered or $n,2n$ neutrons appeared mostly to have energies of less than ~ 3 Mev.

Stelson and Goodman,⁶ using photographic emulsion techniques, measured the distribution in energy of the inelastic neutrons from the interaction of 15-Mev neutrons with lead, iron, and aluminum. Their results confirm those cited above, as do also the results of Whitmore and Dennis⁷ who used similar photographic emulsion techniques to investigate the neutron spectra from 14-Mev neutrons interacting with lead and bismuth.

The method used to obtain the results presented in this paper differs from the method utilized by Phillips *et al.*⁵ in that the material to be investigated surrounds the source instead of the detector, and the neutron spectra are measured with nuclear emulsion techniques in order to obtain better energy resolution and more

* Work performed under the auspices of the AEC.

¹ Barschall, Battat, Bright, Graves, Jorgensen, and Manley, Phys. Rev. **72**, 881 (1947); Barschall, Manley, and Weisskopf, Phys. Rev. **72**, 875 (1947).

² B. T. Feld, Phys. Rev. **75**, 1115 (1949).

³ V. F. Weisskopf, Phys. Rev. **52**, 295 (1937); V. F. Weisskopf and D. H. Ewing, Phys. Rev. **57**, 472 (1940); V. F. Weisskopf, *Lecture Series in Nuclear Physics* (U. S. Government Printing Office, Washington, D. C., 1947); V. F. Weisskopf and J. M. Blatt, MIT Technical Report No. 42 (May 1950) (unpublished).

⁴ Gittings, Barschall, and Everhart, Phys. Rev. **75**, 610 (1949).

⁵ Phillips, Davis, and Graves, Phys. Rev. **88**, 600 (1952).

⁶ P. H. Stelson and C. Goodman, Phys. Rev. **82**, 69 (1950).

⁷ B. G. Whitmore and G. E. Dennis, Phys. Rev. **84**, 296 (1951).

precise values for the cross section for inelastic neutron production as a function of the energy of the inelastic neutron. An inelastic neutron is defined as a neutron produced by interaction of the primary neutron with the target nucleus by any means other than elastic scattering. The threshold detector data permit the determination of only a rough energy distribution for the inelastic neutrons, since only a few suitable detectors are presently available whose thresholds and energy sensitivity have been sufficiently investigated.

II. EXPERIMENTAL METHOD

Figure 1 represents the experimental arrangement. The shell thickness of all the scatterers was chosen to be approximately one-quarter of a mean free path for inelastic collision of 14-Mev neutrons. Neutrons of energy 13.4 to 14.8 Mev were generated by the bombardment of a thick tritium-zirconium target⁸ by a magnetically analyzed molecular beam of 200-kev deuterons. The number of neutrons generated was measured by counting in a proportional counter the He⁴

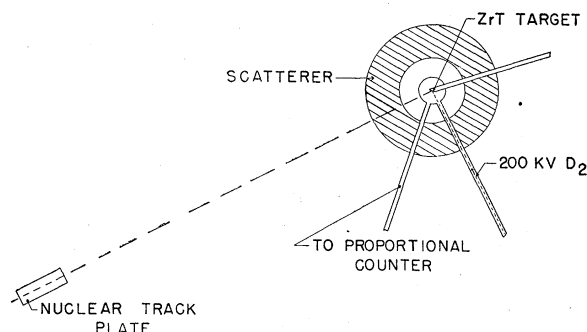


Fig. 1. Schematic view of experimental arrangement.

particles from the $H^3(d,n)He^4$ reaction. Ilford 200- μ C-2 nuclear track plates, the emulsion of each covered by a foil of 0.010-inch platinum, were wrapped in black paper and placed 65 cm from the neutron source. A line through the center of the plates, parallel to the long dimension, intersected the center of the neutron source at an angle of approximately 90° to the direction of the deuteron beam. The maximum angle between a scattered neutron path and the plate axis was $\approx 9^\circ$.

Plates were exposed to neutrons from the bare target assembly to check on the accuracy of absolute neutron counting by the photographic emulsion method and to obtain a background spectrum in the region below the primary peak. Exposures to the source surrounded by thin shells of the various materials were carried out in the same manner as the "background" exposures.

The plates were processed by the "two solution method"⁹ and their analysis carried out under 90X apochromatic objectives and 6X compensating eye-

pieces using Leitz Ortholux microscopes. The microscope stage is fitted with a micrometer screw to which is attached a graduated drum on which one division represents a transverse motion along the screw of 2.5 microns. This adaptation, which was engineered and built by Erb and Gray of Los Angeles, makes possible the measurement of a displacement along the screw axis with an accuracy of approximately ± 3 microns in 1000 microns. For tracks shorter than 50 microns a calibrated eyepiece graticule is used.

For each plate, three to twelve swaths, one cm long by approximately 100 microns wide, were analyzed. The traverses were made in a direction parallel to that of the incident neutrons. All proton tracks originating in the emulsion volume covered by the swaths, which were completely contained within the emulsion within a rectangular pyramid of half-angle 15° in the unprocessed emulsion, were measured. The emulsion volume analyzed was taken at the edge of the plate nearest the source in order to avoid the possibility of attenuation of the neutrons by emulsion, glass backing, and platinum covering. From the ranges of the tracks, corresponding proton recoil energies are deduced, using the range-energy curves of Rotblatt,¹⁰ corrected for water content of the plates on the basis of the range in the emulsion of proton recoils from 14.2-Mev neutrons. The proton recoil energies are transformed to incident neutron energies by the relation $E_p = E_n \cos^2 \theta$, where E_p is the proton energy, E_n is the neutron energy, and θ is the average angle between the incident neutron and the recoil proton in the unprocessed emulsion. θ was determined from the scatterer-detector geometry and angle of acceptance for the recoil protons and was approximately 10° in all cases.

In order to calculate the absolute neutron flux at the detector as a function of energy, it is useful to define the following symbols:

$N(E_p)\Delta E_p \equiv$ number of proton recoils having energy between E_p and $E_p + \Delta E_p$, which are projected from unit emulsion volume and into a given solid angle, $d\Omega$.

$n_0 \equiv$ number of hydrogen atoms per unit emulsion volume.

$\sigma_{n,p}(E_n) \equiv$ neutron-proton scattering cross section as a function of energy. The neutron-proton cross sections were taken from the compilation of Adair.¹¹

$P(l) \equiv$ probability that a track of given length, l , does not leave the emulsion.

Then the flux of neutrons in any given energy interval between E_n and $E_n + \Delta E_n$ is

$$F(E_n)\Delta E_n = \frac{4\pi N(E_p)\Delta E_p}{4P(l)n_0\sigma_{n,p}(E_n)\cos\theta d\Omega} \quad (1)$$

⁸ Graves, Rodrigues, Goldblatt, and Meyer, Rev. Sci. Instr. 20 579 (1949).

⁹ M. Blau and J. de Felice, Phys. Rev. 74, 1198 (1948).

¹⁰ J. Rotblatt, Nature 167, 550 (1951).

¹¹ R. K. Adair, Revs. Modern Phys. 22, 249 (1950).

In compiling the data, ΔE_p was always chosen such that ΔE_n would be 0.5 Mev.

The difficulties involved in making absolute neutron flux measurements with nuclear emulsions have been adequately described and referenced in a paper by Barschall *et al.*¹² The value for n_0 was taken as given by the manufacturer with a small correction for the additional water content due to the relative humidity prevailing during exposure. (Dr. Webb of Eastman Kodak very kindly performed accurate experiments on the variation of water content with relative humidity.)

In the course of attempts to increase the accuracy of the absolute neutron flux measurements, the following procedures were found helpful in the determination of n_0 and $d\Omega$:

(1) The thickness of the emulsion is measured prior to development by removing the emulsion from one or more corners of the plate and measuring the emulsion thickness with a dial indicator. This gives the initial emulsion thickness, which, together with the correction for relative humidity, is used to calculate n_0 .

(2) After development, the emulsion thickness is measured with the fine focus screw of the same microscope which is to be used to analyze the plate. This measurement, along with the measurement referred to in (1), makes possible the use of the fine focus screw to measure track dips and hence to define $d\Omega$, in one dimension, in terms of the undeveloped emulsion thickness. This procedure makes an accurate determination of emulsion shrinkage and an absolute calibration of the microscope fine focusing adjustment unnecessary. It is only necessary that the fine focus screw motion is a linear function of the resultant stage motion within the region in which it is used.

(3) The calculation of $P(l)$ assumes that the tracks proceed in a straight line without suffering scattering. Consequently if the product of the length of tracks and the sin of the angle of acceptance is less than the emulsion thickness, the effective value of $d\Omega$ is less than calculated because of the loss of singly or multiply scattered tracks which undeflected would have remained in the emulsion volume. In the present experiment there were few neutrons between 4 and 12 Mev. Since scattering introduces negligible error in the evaluation of $P(l)$ for neutrons below 4 Mev, ($P(l)$ differs little from unity for 200- μ emulsions at this energy) the procedure was adopted, somewhat at expense of resolution, of permitting a rather large half-angle for track acceptance (15°). This implies that all protons projected by neutrons of energy >12 Mev at an angle of 15° with the neutron direction will leave the top or bottom of the emulsion if they do not scatter. However, those which scatter in such a way as to end in the emulsion will be counted and will to a large extent compensate for the proton recoils which are destined to end within the

emulsion but do not do so as a result of single or multiple scattering.

The absolute flux measurements of high energy neutrons arriving at the detector agree to an accuracy of ± 12 percent, when statistical accuracies are 5 percent or better, with the values calculated from the source strength determined by alpha-counting, the cross section measurements of Phillips *et al.* and the material thicknesses. However, at low energies (≈ 1 Mev) the absolute accuracy is probably not better than ± 20 percent.

From the flux and energy distribution of the inelastic neutrons corresponding to a given flux of primary neutrons, and the number of atoms per cm^2 of scatterer, it is possible to determine the cross section for the production of neutrons as a function of the energy of the emitted neutrons. Let $\sigma(E_0, E_n)$, the differential cross section for the emission of neutrons of energy E_n when the incident neutron energy is E_0 , be defined by

$$\int_{0.5 \text{ Mev}}^{12 \text{ Mev}} \sigma(E_0, E_n) dE_n = \frac{NT_r\sigma_i}{(1-T_r)N_0}, \quad (2)$$

where N is the flux of inelastic neutrons of energy between 0.5 and 12 Mev, N_0 is the flux of neutrons (transmitted) of energy 12 to 15 Mev, T_r is the fraction of the neutrons which have not suffered inelastic collisions and σ_i is the cross section for inelastic collision.⁵ T_r and σ_i are related by

$$T_r = e^{-\sigma_i t}, \quad (3)$$

where t is the number of atoms per cm^2 in the spherical shell. It should be noted that

$$\int_{0.5 \text{ Mev}}^{12 \text{ Mev}} \sigma(E_0, E_n) dE_n$$

may be larger than σ_i because of $n, 2n$ processes.

III. RESULTS

Table I presents all the data obtained on the elements investigated. The rows give consecutively (I) the elements investigated; (II) the wall thickness of each spherical shell used; (III) transmission of 14-Mev neutrons through each shell as calculated from the inelastic cross sections;⁵ (IV) values for transmission as given by the ratio of neutrons above 12 Mev determined from the nuclear plates with and without the scatterer in place; (V) the number of tracks measured for each element; (VI) the total cross section for the emission of neutrons of energy 0.5 to 12 Mev. The lower half of the table gives, for each element investigated, the energy distribution of the neutrons. The neutrons above approximately 12 Mev are transmitted neutrons, i.e., they have not suffered inelastic collision.

The values of σ_i used to evaluate $\int \sigma(E_0, E_n) dE_n$ were taken from reference 5 since those values of σ_i are

¹² Barschall, Rosen, Taschek, and Williams, *Revs. Modern Phys.* **24**, 1 (1952).

TABLE I. Summary of data for the interaction of 14-Mev neutrons with various elements. Row I gives the elements investigated; Row II lists the wall thickness of each spherical shell used; Row III lists the transmission of 14-Mev neutrons through each shell as calculated from the inelastic cross sections (see reference 5); Row IV lists values for transmission as given by the ratio of neutrons above 12 Mev determined from the nuclear plates with and without the scatterer in place; Row V gives the number of tracks measured for each element; Row VI gives the total cross section for the emission of neutrons of energy 0.5 Mev to 12.0 Mev for incident neutrons of E_0 approximately 14 Mev; Row VII gives the results of the calculation of T for each element using Eq. (4); Row VIII gives the values of a obtained from Eq. (6). The lower half of the table gives, for each element investigated, the energy distribution of the neutrons, corrected for background, resulting from the interaction of 14-Mev neutrons with the element. The neutrons above approximately 12 Mev are transmitted neutrons, i.e., they have not suffered collision.

I	Element	C	Al ^a	Fe	Cu	Zn	Ag	Cd	Sn	Au	Pb	Bi
II	$t(10^{24} \text{ atoms/cm}^2)$	0.597	0.223	0.174	0.175	0.169	0.151	0.139	0.130	0.130	0.105	0.0985
III	T_r (reference 5)	0.60 ±0.61	0.79 0.71	0.78 0.76	0.77 0.64	0.77 0.70	0.75 0.78	0.77 0.77	0.78 0.57	0.72 0.64	0.76 0.63	0.78 0.74
IV	T_r (present data)	±0.09	±0.10	±0.11	±0.10	±0.10	±0.12	±0.12	±0.10	±0.10	±0.10	±0.10
V	Number of tracks measured	1500	1884	1020	1031	1344	1039	1012	1035	1166	1108	1496
VI	$\int_{0.5 \text{ Mev}}^{12.0 \text{ Mev}} \sigma(E_0, E_n) dE_n$ (barns)	0.52 ±0.2	0.65 ±0.17	1.3 ±0.3	1.0 ±0.25	1.3 ±0.3	1.6 ±0.4	2.2 ±0.6	1.8 ±0.5	2.1 ±0.5	3.3 ±0.8	3.9 ±1.0
VII	$T = \frac{-d[\ln\{F(E_n)/E_n\}]}{dE_n}$ (Mev)	1.04 ±0.11	1.01 ±0.10	0.76 ±0.08	0.77 ±0.08	0.73 ±0.07	0.63 ±0.06	0.66 ±0.07	0.56 ±0.06	0.66 ±0.07	0.76 ±0.08	0.95 ±0.10
VIII	$a(\text{Mev})^{-1}$	52.0 ±10.0	56.0 ±11.0	98.0 ±20.0	95.0 ±19.0	105.0 ±21.0	143.0 ±29.0	129.0 ±25.0	182.0 ±36.0	129.0 ±25.0	97.0 ±19.0	63.0 ±13.0
Energy (Mev)		Neutron flux $\times 10^{-6}$ (neutrons/cm ²)										
	0.5-1.0	7.7	5.0	11.6	14.2	15.4	27.0	23.5	24.1	25.6	19.5	20.9
	1.0-1.5	8.0	5.1	9.5	8.3	8.4	15.3	17.2	14.3	18.4	25.5	17.3
	1.5-2.0	6.5	4.4	5.9	4.8	6.3	7.8	7.3	8.3	10.3	13.4	13.7
	2.0-2.5	4.1	3.5	5.5	3.7	5.2	6.0	7.9	2.4	6.4	11.0	10.5
	2.5-3.0	4.8	2.0	2.8	3.7	3.2	3.5	4.4	1.7	4.7	7.7	9.2
	3.0-3.5	1.3	1.9	1.6	1.3	1.3	2.5	1.9	1.9	0.4	3.2	6.1
	3.5-4.0	2.6	0.5	1.4	0.0	1.6	0.5	1.0	2.1	0.8	2.9	2.4
	4.0-4.5	2.7	1.4	2.3	2.2	0.9	0.0	2.8	0.6	1.6	1.1	2.5
	4.5-5.0	3.6	1.4	1.5	0.5	1.4	0.0	0.0	0.6	0.7	0.9	2.3
	5.0-5.5	1.9	2.0	0.1	0.8	0.0	0.0	0.6	0.0	0.6	0.0	0.3
	5.5-6.0	0.4	1.1	0.6	0.5	0.9	1.3	0.8	0.0	0.2	0.3	0.5
	6.0-6.5	2.2	0.7	0.0	0.2	1.6	1.1	0.7	0.2	0.9	0.0	0.4
	6.5-7.0	2.1	0.9	0.4	0.5	1.7	0.3	1.3	0.3	0.0	1.1	1.2
	7.0-7.5	5.0	0.9	0.0	0.0	0.3	0.0	0.1	0.2	0.7	0.2	1.6
	7.5-8.0	1.2	0.3	0.0	0.0	2.0	0.0	0.4	0.3	0.0	0.8	0.9
	8.0-8.5	3.0	0.3	1.0	0.5	0.6	0.5	0.0	0.0	1.3	0.3	0.4
	8.5-9.0	4.0	0.8	0.0	0.0	0.0	0.0	1.3	0.0	0.8	0.0	0.0
	9.0-9.5	3.3	0.2	0.4	0.0	0.1	0.0	0.3	0.6	0.0	0.6	2.4
	9.5-10.0	6.3	2.6	0.9	1.0	1.0	0.0	1.3	0.8	0.0	0.5	0.4
	10.0-10.5	1.3	1.2	0.6	0.7	2.2	0.9	2.6	0.0	1.4	2.1	1.0
	10.5-11.0	3.0	1.7	0.0	0.4	1.3	1.5	0.0	0.0	1.5	0.8	1.2
	11.0-11.5	2.6	0.0	0.0	0.0	0.6	0.0	1.3	0.7	0.0	2.0	0.0
	11.5-12.0	5.4	0.0	0.0	0.0	0.0	0.7	0.0	0.0	0.0	0.4	0.0
	12.0-12.5	4.7	5.9	1.6	0.9	1.0	0.0	1.5	0.0	0.0	1.0	3.5
	12.5-13.0	13.8	10.4	5.9	8.8	1.4	0.8	1.7	6.1	5.8	0.0	3.0
	13.0-13.5	35.7	22.8	21.8	14.0	20.1	20.1	12.8	12.2	15.6	12.6	17.6
	13.5-14.0	60.9	57.9	59.1	47.7	56.1	59.1	63.8	54.5	85.0	55.5	72.0
	14.0-14.5	85.2	91.8	77.9	99.1	102.3	128.8	118.9	83.6	98.4	97.4	104.1
	14.5-15.0	7.3	10.4	7.2	18.8	22.4	36.1	29.2	7.3	11.0	21.9	11.4

^a Contains 2.5 atomic percent copper.

considerably more accurate than the values obtainable from this experiment. σ_i for Ag and Sn were interpolated from the empirical relationship between σ_i and the atomic weight.

The data given in Table I have been corrected for background. These corrections were made on the basis of the runs without scatterer and on the assumption that the ratio of the background neutrons to the neutrons of energy 12 to 15 Mev is not significantly altered by the presence of the scatterer.

IV. DISCUSSION

The statistical theory of Weisskopf and co-workers³ is applicable to interactions of neutrons with nuclei under the conditions that the incident neutron interacts with all the nucleons of the target nucleus and the incident neutron energy is large compared to the level spacing of the residual nucleus in the region of maximum excitation produced by the interaction. It is predicted

that the energy distribution of the inelastically scattered neutrons is Maxwellian and is given by

$$[d\sigma(E_0, E_n)/dE_n]dE_n = \text{const} \times E_n \sigma_c e^{-E_n/T} dE_n, \quad (4)$$

where $d\sigma(E_0, E_n)/dE_n$ is the differential cross section per unit energy interval for the scattering of incident neutrons of energy E_0 into the energy interval between E_n and E_n+dE_n , σ_c is the cross section for the formation of a compound nucleus, and T is a parameter which is analogous to a temperature, at an excitation energy of E_0 of the residual nucleus and will be called the temperature. This implies, assuming that T does not vary with E in the energy region in which Eq. (4) obtains, that

$$\ln \left[\frac{1}{E_n} \frac{d\sigma(E_0, E_n)}{dE_n} \right] \text{ vs } E_n$$

should give a straight line of negative slope $1/T$, that

the mean energy of the inelastic neutrons is $2T$, and that the maximum intensity occurs at T .

According to the theory, if the maximum energy of the residual nucleus after $n, 2n$ reaction is high enough, it may be expected that the energy of the second neutron emitted will have a Maxwellian distribution characterized by a constant $T(E_0 - \Delta)$, where Δ is the binding energy of the second neutron, which temperature is associated, not with the target nucleus but with the residual nucleus after the $n, 2n$ reaction. Hence the function $F(E_n)/E_n$ will be the sum of two exponentials, the relative proportion of each governed by the ratio of the number of inelastic scattering reactions to $n, 2n$ reactions. The resolution obtained in the present experiment is probably not good enough to separate two exponentials if they were present. For equal probability of inelastic scattering and $n, 2n$ reaction from a medium

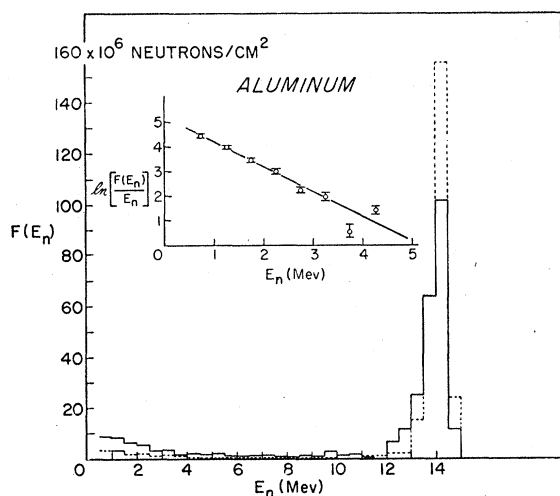


FIG. 2. Neutron spectrum from Al. Solid line represents the energy distribution of the neutrons from the source surrounded by Al sphere; broken line represents the distribution from source alone. The inset is a semilogarithmic plot of the inelastic neutron distribution divided by the neutron energy *vs* neutron energy. Background has been subtracted.

weight element, an apparent T approximately 20 per cent lower than T for first neutron emission would be deduced. In any case the value of T deduced from the data will be a lower limit of T for the target nucleus associated with inelastic scattering.

The values of T deduced from the data are given in row VII of Table I. Figs. 2, 3, and 4 are typical of the spectra obtained. The insets show

$$\ln[F(E_n)/E_n] \text{ vs } E_n,$$

indicating to what extent the neutron distributions are Maxwellian. None of the elements investigated appeared to show evidence of a second exponential component. There are a measurable number of neutrons above 5 Mev and these do not follow the exponential which fits the lower energy neutrons. The number of neutrons

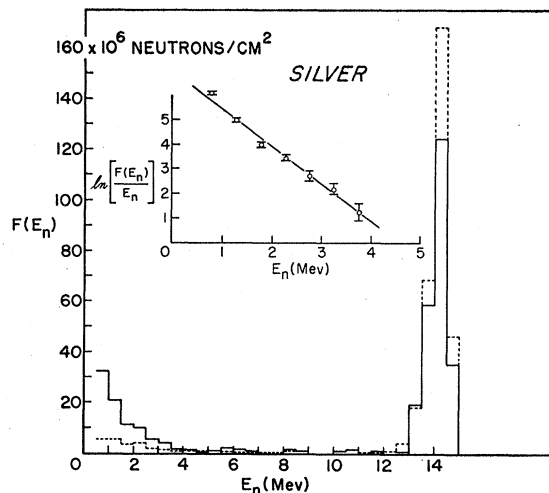


FIG. 3. Neutron spectrum from Ag. Solid line represents the energy distribution of the neutrons from the source surrounded by Ag sphere; broken line represents the distribution from source alone. The inset is a semilogarithmic plot of the inelastic neutron distribution divided by the neutron energy *vs* neutron energy. Background has been subtracted.

above 4 Mev appears to increase with decreasing mass number. It must be emphasized that for carbon, and perhaps even for aluminum, Eq. (4) would not be expected to hold from the very nature of the assumptions upon which it is based.

Stelson and Goodman, applying the statistical analysis, obtained values for T of 1.1, 0.6, and 0.7 Mev for Al, Fe, and Pb, respectively. Whitmore and Dennis obtained temperatures of 0.8 and 0.9 Mev for Pb and Bi, respectively. As can be seen from Table I, our results on these three elements are in quite good agreement with theirs. Stelson and Goodman used scatterers which

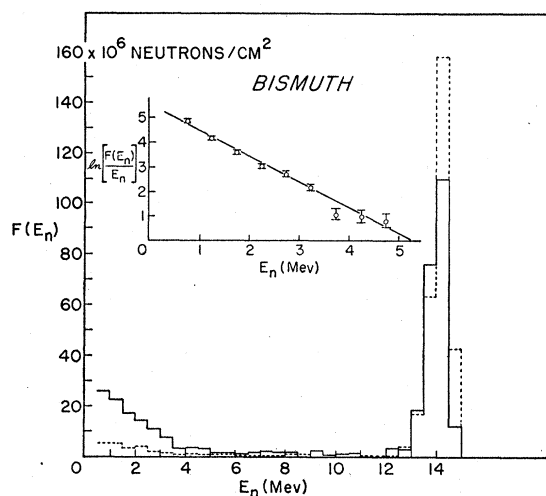


FIG. 4. Neutron spectrum from Bi. Solid line represents the energy distribution of the neutrons from the source surrounded by Bi sphere; broken line represents the distribution from source alone. The inset is a semilogarithmic plot of the inelastic neutron distribution divided by the neutron energy *vs* neutron energy. Background has been subtracted.

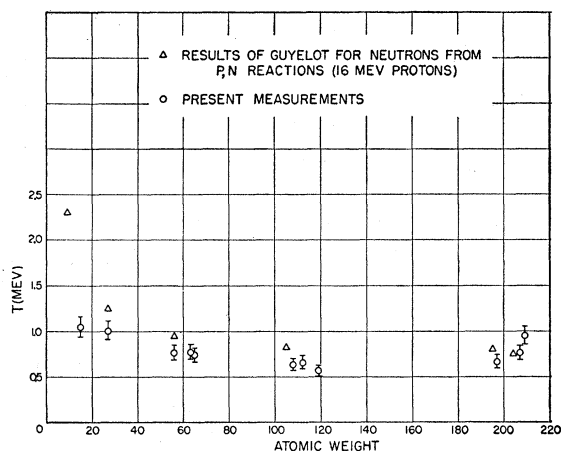


FIG. 5. Variation of T with mass number. Gugelot should read Gugelot.

had a thickness of one mean free path (1λ) for inelastic collision, Whitman and Dennis used scatterers of $\frac{1}{2}\lambda$ thickness, and in the present experiment the scatterers were of thickness $\frac{1}{4}\lambda$.

On the assumption of an inelastic cross section which is independent of the primary neutron energy it may be shown that for a thickness of $\frac{1}{2}\lambda$ approximately 25 to 45 percent of the inelastically scattered neutrons have had more than one inelastic collision. For a thickness of $\frac{1}{4}\lambda$ this fraction drops to approximately 15 to 20 percent. However, the inelastic cross section for Pb and Bi for 1–3 Mev neutrons is less than one-third of its value for 14-Mev neutrons. A study of the data leads to the conclusion that the neutron spectrum for Pb will not be appreciably affected by the difference in sample thickness in the various experiments. For Fe, measured by Stelson and Goodman and in the present work, the difference between 1λ and $\frac{1}{4}\lambda$ scatterers by the same analysis may be expected to be not large. Also the dearth of low energy neutrons reduces the accuracy of the measurements, so that smaller differences would go undetected. Aluminum has zero inelastic cross section for lower energies so that the spread in scatterer thickness should not cause large differences in results for this element.

In developing the statistical theory of nuclear reactions the assumption is made that the mode of disintegration of the compound nucleus depends only upon the excitation energy and angular momentum and is independent of the method of formation. This implies that the neutron spectra from (p,n) reactions should not differ appreciably from the energy distributions of neutrons from (n,n) processes, provided the compound nuclei and their excitation energies are the same.

Gugelot¹³ has determined the variation of nuclear temperature, T , with mass number for a large number of elements by measuring the neutron spectra resulting from (p,n) reactions for 16-Mev protons. Figure 5 is a plot of both his results and those presented here. No attempt has been made to correct for the fact that excitation energies produced by 16-Mev protons are not precisely the same as by 14-Mev neutrons. Gugelot's T values have been adjusted by him for contributions from postulated second neutrons while the present data have not been so treated. It is to be seen, however, that with the exceptions of the low masses, the values of T from the two sets of experiments are in quite good agreement.

According to the statistical theory, the neutron energy distribution $F(E_n)/E_n$ is, to a first approximation, proportional to the level density function $W(E_0 - E_n)$ which describes the density of levels in the residual nucleus as a function of excitation energy $(E_0 - E_n)$, i.e.,

$$W(E_0 - E_n) = F(E_n)/E_n = \text{const} \times \exp\{[a(E_0 - E_n)]^{\frac{1}{2}}\}. \quad (5)$$

For all of the elements investigated, a plot of

$$\ln[F(E_n)/E_n] \text{ vs } (E_0 - E_n)^{\frac{1}{2}}$$

gives a straight line and hence the value of a in the level density function. An equivalent result is obtained by setting

$$T = (4E_0/a)^{\frac{1}{2}}, \quad (6)$$

where T is defined by Eq. (4). The values of a are given in row VII of Table I. These, with Eq. (5) suffice to determine the relative level densities of the elements investigated for a given excitation energy. The values of a , do not increase smoothly with increasing mass number as would be predicted on the basis of statistical theories.

The concept of the statistical theory that the energy introduced into the nucleus is shared by all the particles is equivalent to a requirement that T be a decreasing function of the atomic weight A . However, T appears to be essentially independent of A . Correction for the effect of $n,2n$ reactions can only raise the values of T for high values of A which is an even greater departure from prediction. It is concluded that the simple sharing of energy by all the particles of the nucleus is not supported by the results of the present experiment.

The authors are indebted to R. W. Davis for work with the 14-Mev neutron source and to Pat Agee, May Bergstresser, and Pearl Norwood for analysis of the plates and for much of the computing work involved in the reduction of the data.

¹³ P. C. Gugelot, Phys. Rev. **81**, 51 (1950).